**Structural and Multidisciplinary Optimization manuscript No.**
(will be inserted by the editor)

# Truss geometry and topology optimization with global stability constraints

Alemseged Gebrehiwot Weldeyesus · Jacek Gondzio · Linwei He · Matthew Gilbert · Paul Shepherd · Andrew Tyas

Received: date / Accepted: date

**Abstract** In this paper, we introduce geometry optimization into existing topology optimization of truss structures with global stability constraints. The design variables are the cross-sectional areas of the bars, and the coordinates of the joints. This makes the optimization problem formulations highly nonlinear and yields nonconvex semidefinite programing problems, for which, there are only limited available solvers when compared to that of other classes of optimization problems. In this study, we present problem instances of truss geometry and topology optimization with global stability constraints that have been solved using a standard primal-dual interior point implementation. During the solution process, both the the cross-sectional areas of the bars and the coordinates of the joints are concurrently optimized. Additionally, we apply adaptive optimization techniques to allow the joints to navigate larger move limits and improve the quality of the optimal designs.

**Keywords** Geometry and topology optimization · Global stability · Nonlinear semidefinite programming · Interior point methods

A.G. Weldeyesus
School of Mathematics and Maxwell Institute for Mathematical Sciences The University of Edinburgh, Peter Guthrie Tait Road, Edinburgh EH9 3FD, United Kingdom.

J. Gondzio
School of Mathematics and Maxwell Institute for Mathematical Sciences The University of Edinburgh, Peter Guthrie Tait Road, Edinburgh EH9 3FD, United Kingdom.

L. He
Department of Civil and Structural Engineering, University of Sheffield, Sir Frederick Mappin Building Mappin Street, Sheffield, S1 3JD, United Kingdom.

M. Gilbert
Department of Civil and Structural Engineering, University of Sheffield, Sir Frederick Mappin Building Mappin Street, Sheffield, S1 3JD, United Kingdom.

P. Shepherd
Department of Architecture and Civil Engineering, University of Bath, Claverton Down, Bath BA2 7AY, United Kingdom.

A. Tyas
Department of Civil and Structural Engineering, University of Sheffield, Sir Frederick Mappin Building Mappin Street, Sheffield, S1 3JD, United Kingdom.

## 1 Introduction

Truss design problems are often formulated based on the so-called ground structure approach [12], in which a set of joints are distributed in the design space and are connected by some potential bars. We are concerned with a truss design problem where the goal is to optimize both the topology and geometry of the structures, i.e, when the design variables are the cross-sectional areas of the bars and the coordinates of the joints. These problems have been studied in many articles, for example [11,25,7,9,36,40,1,46,32], to mention just a few. The problems are highly nonlinear, mainly due to the variation of the coordinates of the joints. However, the models are known to obtain optimal designs that are more efficient and practically relevant designs, requiring less post-processing tools, using a small number of joints and connecting bars in the design space. On the contrary, one can also obtain efficient (least weight) structures by considering many more joints, but fixed, and solving large-scale linear/ nonlinear topology optimization problems [8,22,16, 41]. However, the resulting designs usually have many active joints and bars, and could be far from practical.
Due to the high nonlinearity of the geometry and topology optimization problem formulations, several solution techniques have been proposed, mainly to improve the computation tractability of the problems [21,37,45,28,3,20]. One of the most common techniques is to use the so-called alternating method, for example in [37,28], where the prob-

lems are solved for a fixed geometry but with variation in topology and vice-versa. These techniques usually obtain good designs, but in some cases they may not fulfil optimality conditions. In other studies, the topology and geometry of the structure are optimized simultaneously, see [3], and it has been proved that the solution is (local) optimal. In both approaches, some studies also use first-order information [45], while others attempt to use the second-order primal-dual method [21,20] to improve convergence properties. For an overview of these approaches and other solution strategies, we refer the reader to [3].

Many studies on the optimization of truss structures incorporate far more constraints than the classical formulations, where the weight is minimized with constraints on the compliance or the other way round, to improve the practicality of the optimal designs. These include constraints on stresses and/or on local buckling based on Euler's formula [24,18, 43,44,56,2,38,19,17,31], constraints with nodal stabilities based on nominal forces [49,10], and constraints with global stabilities [6,29,42,13,48]. Thee are also variants of these formulations incorporating buckling constraints using frame structures [47,33], beam modeling [30], and continuum structures [14].

In this paper, we address truss design problems with global stability constraints formulated as nonlinear semidefinite programming. Such problems have been extensively studied in [6,29,26,42,13] and solved, for example by [15,27], but all for fixed joints. In [51], an invariant large-scale problem formulation to those in [26], obtained by relaxing nonlinear kinematic compatibility constraints, but still for fixed joints, has been solved using a customized primal-dual interior point method by exploiting sparsity and low-rank properties of the associated element stiffness matrices [9,5,4,8], the use of column generation procedure (member adding) [16,41,50], and a warm-start strategy [50].

The goal of this problem is to introduce geometry optimization to existing truss topology optimization with global stability constraints via nonlinear semidefinite programming, in particular to models proposed in [26,50], and to show that there are problems of this type which can be solved using a standard primal-dual interior point method. This is a surprise, considering the severity of the nonlinearity and nonconvexity of the problem formulations. We refer the reader to [53] for a recent survey of numerical methods for nonlinear semidefinite programming, and further discussions on how the field is still generally challenging.

One drawback of the solutions obtained by applying geometry optimization is that the resulting optimal designs depend hugely on the initial positions and number of the joints. As an attempt to overcome this, and another challenge associated with numerical instability, namely when some joints come too close to each other leading to singularity, we perform adaptive geometry and topology optimization, inspired by [20]. This is an iterative procedure where the problems are initially solved by restricting the movement limits of the joints to smaller regions, and then progressively updating them. With this approach, the joints can ultimately navigate larger regions, which could be far beyond the design space defined by the initial joint configuration. During the procedure, inactive joints, i.e., the joints connected entirely to thin bars that have cross-sectional areas below a prescribed threshold, are removed. Moreover, we perform some of the common techniques in geometry optimization such as node merging when the joints are too close, and node melting when a joint just connects at the cross points two active collinear bars. The overall procedure can amount to a certain extent to a post-processing or rationalization of optimal truss designs [20].

The paper is organized as follows. In Section 2, we present the essential mathematical background for geometry optimization of trusses. In Section 3, the truss geometry and topology optimization with global stability constraints problem formulation, modelled as nonlinear semidefintie programming, is presented. We describe the general framework of the primal-dual interior point method in Section 4. The numerical experiments and adaptive geometry and topology optimization are described in Section 5. Finally, the conclusions and future research directions are listed in Section 6.

## 2 Background

In this section, we describe the essential mathematical concepts which are useful for modelling truss geometry and topology optimization with global stability constraints. Part of this section closely follows [52] and [26]. We adopt the ground structure approach [12], i.e., a finite set of joints are distributed in a given $N$-dimensional design space, where $N \in \{2,3\}$, and the joints are connected by some potential bars. Let $d$ be the number of the joints with $\bar{v}_j, j = 1,...,d$ the corresponding coordinates of the positions of the joints. Hence, $\bar{v}_j = (x_j, y_j)$ if $N = 2$, and $\bar{v}_j = (x_j, y_j, z_j)$ if $N = 3$. Note that these coordinates will be considered as initial positions of the joints in this paper. Let $m$ be the number of bars with the cross-sectional areas $a_i$, $i = 1,...,m$. In geometry optimization, the joints are allowed to move within certain limits, we refer the reader to [3,20] for a brief discussion on various types of admissible move limits. Throughout the course of the paper, we assume that the supported and loaded joints are always fixed, and the other joints, say $d_0$, are allowed to move within a move limit defined by the neighbourhood

$$\mathscr{V} = \mathscr{V}_1 \cap \mathscr{V}_2 \tag{1}$$

where $\mathscr{V}_1$ is a region defined by balls of radii $r$ around the joints and is given by

$$\mathscr{V}_1 = \{v \in \mathbb{R}^{d_0 N} | \, ||v_j - \bar{v_j}||^2 \leq r_j^2, \; j = 1, ..., d_0\}, \tag{2}$$

where $||\cdot||$ is the Euclidean norm, and $\mathscr{V}_2$ is a region described by a set of linear constraints when the joints are required to remain, for example, within the given design domain. Hence, it can be defined by

$$\mathscr{V}_2 = \{v \in \mathbb{R}^{d_0 N} | v_{j,k}^{min} \leq v_{j,k} \leq v_{j,k}^{max}, \; j = 1, ..., d_0 . \, k = 1, ..., N\}. \tag{3}$$

Note that, we have $d_0 < d$. In order to avoid singularity (or non-differentiability, example when $v_i^{(2)} = v_i^{(1)}$ in (5)), the radius $r_j$ of each of the balls in (2) is chosen to satisfy

$$0 < r_j = \frac{1}{2} \min\{||\bar{v}_j - v_p||, \; p \in I\} - \varepsilon, \tag{4}$$

where $I$ is the set of indices of the joints connected to joint $j$, and $\varepsilon > 0$.
Let $v_i^{(1)}$ and $v_i^{(2)}$ denote the coordinates of the start and end joints of the bar $i$, $i = 1, ..., m$. Then, its length $l_i(v)$ is given by

$$l_i(v) = ||v_i^{(2)} - v_i^{(1)}||, \tag{5}$$

and let $(-\gamma_i^e(v), \gamma_i^e(v))^T$ be the non-zero entries of the associated vector of direction cosines $\gamma_i(v) \in \mathbb{R}^n$, where

$$\gamma_i^e(v) = \frac{1}{l_i(v)} (v_i^{(2)} - v_i^{(1)})^T. \tag{6}$$

Now, given an external load $f \in \mathbb{R}^n$, $n \approx Nd$, the resulting displacement $u \in \mathbb{R}^n$ satisfies the (linear) elastic equilibrium equation

$$K(a, v) u = f, \tag{7}$$

where the stiffness matrix $K(a, v)$ is computed as

$$K(a, v) = \sum_{i=1}^{m} a_i \frac{E}{l_i(v)} \gamma_i(v) \gamma_i^T(v), \tag{8}$$

with $E$ being the Young's modulus of the material.
Next, we define the so-called geometrical stiffness matrix $G(a, v, u)$ as given by

$$G(a, v, u) = \sum_{i=1}^{m} \frac{a_i E \gamma_i(v)^T u}{l_i^2(v)} (\delta_i(v) \delta_i(v)^T + \eta_i(v) \eta_i(v)^T). \tag{9}$$

The vectors $\delta_i(v)$, and $\eta_i(v)$ are determined so that $\gamma_i(v)$, $\delta_i(v)$, and $\eta_i(v)$ are mutually orthogonal [26], and hence there are many possible ways of choosing these vectors. When all of the joints are fixed, i.e., when solving topology optimization, these have been computed as the orthogonal basis of the null space of $\gamma_i^T$ in [26]. We follow similar approach but additionally derive the vectors $\delta_i(v)$ and $\eta_i(v)$ explicitly as described in Subsection 2.1 since we need to compute the derivatives of these vectors with respect to the coordinates of the joints during the optimization process.

### 2.1 Computing the vectors $\delta_i(v)$, and $\eta_i(v)$

When $N = 2$, (in this case, there is no $\eta_i(v)$), then we have

$$\delta_i^e(v) = A_{2\times 2} \gamma_i^e(v), \tag{10}$$

where the rotation matrix $A_{2\times 2}$ is given by

$$A_{2\times 2} = \begin{pmatrix} 0 & -1 \\ 1 & 0 \end{pmatrix}. \tag{11}$$

In this case, the set $\{\gamma_i^e(v), \delta_i^e(v)\}$ is an orthonormal basis for $\mathbb{R}^2$.
When $N = 3$, first let us define the following three rotation matrices,

$$A_{3\times 3}^{(1)} = \begin{pmatrix} 0 & 0 & 0 \\ 0 & 0 & -1 \\ 0 & 1 & 0 \end{pmatrix}, \; A_{3\times 3}^{(2)} = \begin{pmatrix} 0 & 0 & -1 \\ 0 & 0 & 0 \\ 1 & 0 & 0 \end{pmatrix}, \\ A_{3\times 3}^{(3)} = \begin{pmatrix} 0 & -1 & 0 \\ 1 & 0 & 0 \\ 0 & 0 & 0 \end{pmatrix}. \tag{12}$$

Then, we determine the non-zero entries of $\delta_i(v)$ and $\eta_i(v)$ using the following steps.

Step 1 Compute $\delta_i^e(v)$ as

$$\delta_i^e(v) = \frac{A_{3\times 3}^{(j)} \gamma_i^e(v)}{||A_{3\times 3}^{(j)} \gamma_i^e(v)||}, \tag{13}$$

where $j$ is the index of $|(\gamma_i^e(v))_j|$ with smallest magnitude.

Step 2 Compute $\eta_i^e(v)$ using the vector product

$$\eta_i^e(v) = \gamma_i^e(v) \times \delta_i^e(v). \tag{14}$$

*Remark 1* In the implementation, we use $j = 1$ in Step 1 if $|(\gamma_i^e(v))_1| = |(\gamma_i^e(v))_2| = |(\gamma_i^e(v))_3|$.

Next, we present Proposition 1 just for completeness even though the result follows from basic linear algebra.

**Proposition 1** *Let $N = 3$. Let the vectors $\delta_i^e(v)$ and $\eta_i^e(v)$ be given as in (13) and (14), respectively. Then, the following statements hold.*

*(a) $\delta_i^e(v) \neq 0$, i.e., the vector $\delta_i^e(v)$ has at least one non-zero component.*
*(b) There does not exist a scalar $\alpha \in \mathbb{R}$ such that $\delta_i^e(v) = \alpha \gamma_i^e(v)$.*
*(c) The set $\{\gamma_i^e(v), \delta_i^e(v), \eta_i^e(v)\}$ form an orthonormal basis for $\mathbb{R}^3$.*

*Proof*

(a) This follows from the fact that $\gamma_i^e(v) \neq 0$, see (6), and by construction, we drop the element with the smallest absolute value in $\gamma_i^e(v)$ to form $\delta_i^e(v)$.

(b) This can be easily versified by showing that $\langle \gamma_i^e(v), \delta_i^e(v) \rangle = 0$, i.e., the non-zero unit vectors $\gamma_i^e(v)$ and $\delta_i^e(v)$ are orthogonal.
(c) This follows from (b) and the use of the vector product to form (14).

*Remark 2* We compute $\delta_i^e(v)$ as given in (13), i.e., keep the two largest absolute value entries, to ensure robustness.

## 3 The problem formulation

In this section, we present the problem formulation for the minimum weight truss geometry and topology optimization with global stability constraints which is

$$\begin{aligned} \underset{a,v,u}{\text{minimize}} \quad & l(v)^T a \\ \text{subject to} \quad & f^T u \le \zeta \\ & K(a,v)u = f, \qquad \forall i \\ & K(a,v) + \tau G(a,v,u) \succeq 0 \\ & v \in \mathscr{V} \\ & a \ge 0, \end{aligned} \tag{15}$$

where $\varsigma$ is a given bound on the compliance, the set $\mathscr{V}$ is as in (1), and the design load factor $\tau$ should be at least 1. In that case, the obtained optimal design is stable for the load $\tau f$.

*Remark 3* Problem (15) can be considered as a natural extension of the model in [26], where it is formulated only for topology optimization with global stability constraints, i.e., all nodal coordinates (or joints) are fixed.

*Remark 4* In [50], a variant formulation of (15) written based on member forces has been addressed for fixed joints. After relaxing nonlinear constraints, it is shown that the problem can be solved for a very large number of bars by applying adaptive method, i.e., a technique in which a sequence of much smaller problems are solved to obtain the solution of the original large-scale problem. The computational gain is remarkable and the qualities of the solution of the relaxed problem are good. However, since the joints are fixed, a large number of nodes is still required to obtain least weight structures. This can produce many active joints and bars in the optimal design.

Problem (15) is a highly nonlinear and noncovex semidefinite program and is very difficult to solve [53]. To the best of the authors knowledge, there is no documented literature reporting any solution to the problem.
As mentioned in Section 1, it is in generally a challenge to solve truss geometry and topology optimization with or without stability constraints. In many studies, the so-called alternating optimization approach is used where the optimization problem is split into two problem instances, i.e, fixing joints and optimizing with respect to the cross-sectional areas of the bars, and vice versa [37,28]. The approach is rather heuristic and just aims to reduce the mathematical complexity of the problems, and often obtains good designs. However, these designs do not necessarily satisfy any optimality conditions [3]. The other approach is to solve the problem simultaneously and obtain some local solutions [3]. In this paper, we solve problem (15) simultaneously for both geometry and topology optimization, using a second-order primal-dual interior-point method for nonlinear semidefinite programming described below, i.e. in Section 4.

## 4 The primal-dual interior point framework

In this section, we present an overview of the interior point method and an algorithm we applied to solve problem (15), which is in some sense similar to Section 3 of [52], except some slight reformulation of the general nonlinear semidefinite programming and associated notations, now adopted from [54]. This is to make the flow of the presentation consistent with the notion of this paper. See also [42].
Consider the nonlinear semidefinite programming of the form

$$\begin{aligned} \underset{x\in\mathbb{R}^m}{\text{minimize}} \quad & f(x) \\ \text{subject to} \quad & g(x) = 0 \\ & \mathscr{A}(x) \succeq 0. \end{aligned} \tag{16}$$

The functions $f : \mathbb{R}^m \to \mathbb{R}$, $g : \mathbb{R}^m \to \mathbb{R}^k$, and $\mathscr{A} : \mathbb{R}^m \to \mathbb{S}^n_+$ are assumed to be sufficiently smooth, and $\mathbb{S}^n_+$ is the cone of positive semidefinite matrices in the space $\mathbb{S}^n$ of symmetric $n \times n$ matrices.
After introducing a barrier parameter $\mu > 0$, the associated barrier problem is

$$\begin{aligned} \underset{x\in\mathbb{R}^m}{\text{minimize}} \quad & f(x) - \mu \ln(\det(\mathscr{A}(x)) \\ \text{subject to} \quad & g(x) = 0. \end{aligned} \tag{17}$$

The Lagrangian to problem (17) is

$$\mathscr{L}_\mu(x,\lambda) = f(x) - \mu \ln(\det(\mathscr{A}(x)) + \lambda^T g(x),$$

where $\lambda \in \mathbb{R}^k$ is a Lagrangian multiplier. Introducing the additional matrix variable $Z := \mu(\mathscr{A}(x))^{-1}$, we have

$$\nabla_x \mathscr{L}_\mu(x,\lambda) = \nabla_x f(x) - \mathscr{G}(x)Z + \nabla_x g(x)^T \lambda \tag{18}$$

where

$$\mathscr{G}(x)Z = \begin{pmatrix} \langle \frac{\partial \mathscr{A}(x)}{\partial x_1}, Z \rangle \\ \vdots \\ \langle \frac{\partial \mathscr{A}(x)}{\partial x_m}, Z \rangle \end{pmatrix}. \tag{19}$$

Then, first-order optimality conditions of the barrier problem (17) are

$$\nabla_x \mathscr{L}_\mu(x,\lambda) = 0 \tag{20a}$$
$$g(x) = 0 \tag{20b}$$
$$\mathscr{A}(x)Z - \mu I = 0. \tag{20c}$$

To apply the Newton method to solve the system of nonlinear equations (20), first we need to maintain symmetry, which is done by replacing equation (20c) with

$$H_P(\mathscr{A}(x)Z) = \mu I, \tag{21}$$

where the linear operator $H_P : \mathbb{R}^{n\times n} \to \mathbb{S}^n$, introduced in [55] is defined as follows:

$$H_P(Q) := \frac{1}{2}\left(PQP^{-1} + (PQP^{-1})^T\right)$$

with $P \in \mathbb{R}^{n\times n}$ being some non-singular matrix. There are various ways to choose the matrix $P$. In this paper, we use NT direction [34,35].
Now, to get the search directions $(\Delta x, \Delta\lambda, \Delta Z)$, we can apply the Newton method to (20) with the last equation replaced by (21), and solve the system

$$\begin{aligned} \nabla^2_{xx}\mathscr{L}_\mu(x,\lambda)\Delta x - \mathscr{G}(x)\Delta Z + \nabla_x g(x)^T \Delta\lambda &= -\nabla_x \mathscr{L}_\mu(x,\lambda) \\ \nabla_x g(x)\Delta x &= -g(x) \\ \mathscr{E}\Delta X + \mathscr{F}\Delta Z &= \mu I - H_P(\mathscr{A}(x)Z), \end{aligned} \tag{22}$$

where $\mathscr{E} = \mathscr{E}(x,Z)$ and $\mathscr{F} = \mathscr{F}(x,Z)$ are the derivatives of $H_P(\mathscr{A}(x)Z)$ with respect to $x$ and $Z$, and $\Delta X = \sum_{i=1}^m \Delta x_i \frac{\partial \mathscr{A}(x)}{\partial x_i}$.
The overview of the interior point method is summarized in Algorithm 1. It has two loops. The norm of the optimality conditions in (22) is the stopping criteria, with $\mu = 0$ for the outer loop and $\mu = \mu_k$ for the inner loop. The parameters $\alpha$ and $\sigma$ control step-length of search directions and the centrality of the points, respectively.

**Algorithm 1** The outline of the interior-point method

Choose $(x^0, \lambda^0, Z^0)$ and $\mu_0 = \frac{1}{n}\langle \mathscr{A}(x^0), Z^0\rangle$.
Set the outer iteration counter $k \leftarrow 0$.
**while** stopping criteria is not satisfied **do**
  Set the inner iteration counter $i \leftarrow 0$.
  **while** stopping criteria is not satisfied when $\mu = \mu_k$ **do**
    Compute $(\Delta x^{k,i}, \Delta\lambda^{k,i}, \Delta Z^{k,i})$ by solving system (22).
    Compute a step length $\alpha$ satisfying positiveness (definite) of variables.
    Update $(x^{k,i+1}, \lambda^{k,i+1}, Z^{k,i+1}) \leftarrow (x^{k,i}, \lambda^{k,i}, Z^{k,i}) + \alpha(\Delta x^{k,i}, \Delta\lambda^{k,i}, \Delta Z^{k,i})$.
    $i \leftarrow i+1$.
  **end while**
  Update $\mu_{k+1} := \sigma\frac{1}{n}\langle \mathscr{A}(x^{k,i}), Z^{k,i}\rangle$.
  $k \leftarrow k+1$.
**end while**

## 5 Numerical results

The interior point method has been implemented in MATLAB (R2018a). All numerical experiments have been performed on PC equipped with an Intel(R) Core(TM) i5-8350U CPU running at 1.90 GHz with 8 GB RAM. In all examples, we use input data without units. We use the values of Young's modulus $E = 1$ and the design loading factor $\tau = 1$. In the plots showing optimal designs, only the bars with cross-sectional area $\geq 0.001 a_{\max}$ are shown. The dark dots are the active joints connecting these bars.
In Algorithm 1, mostly we use$\sigma = 0.5$ and $\alpha = 0.8\alpha_{max}$, where $\alpha_{max}$ is the maximum step length such that the current point is positive (definite).

### 5.1 Fixed versus moving joints

In this section, we preset two examples to demonstrate the use of geometry optimization (allowing the joints to move) in reducing the weight of the optimal design. This is done by making comparisons between solutions obtained with fixed and moving joints. Moreover, even though it is not the main purpose the paper, we also demonstrate the usefulness of global stability constraints in these examples, for the sake of completeness. We do this by comparing designs obtained with and without stability constraints.

*Example 1* We start with the L-shaped truss problem shown in Figure 1a that has 132 members which has been solved in [29] for fixed joints. It has dimensions $1\times 3\times 4$ (excluding the region of dimensions $1\times 2\times 3$) and the loads are $(0,0,-0.001)$ each, applied simultaneously. The bound on the compliance is $\varsigma = 0.0005$. When solving the topology optimization problem for fixed geometry and without stability constraints, we get the design in Figure 1b, consisting of two disjoint parallel planar trusses of weight 7.6880. Now, including the stability constrains and solving the problem, again for fixed joints, we obtain the design in Figure 1c, where connectivity between the parallel planar trusses is established. In this case, the design's weight is 7.8340. Next, we allow the joints to move. In this case, we consider the two scenarios below.

(i) The joints are allowed to move in a ball of radius $r = 0.4$, but still remain within the design space of Figure 1a. We obtain the design in Figure 1d that has weight 7.1557 which is reduced by approximately 9% in comparison with of the solution obtained with fixed joints in Figure 1c. Moreover, there is an arch like structure in Figure 1d around the lower surface which spans further around the outer corner.
(ii) The joints are allowed to move in a ball of radius $r = 0.4$, but only the joints in the inner most surfaces are forced to remain within the design space of Figure 1a. In this case,

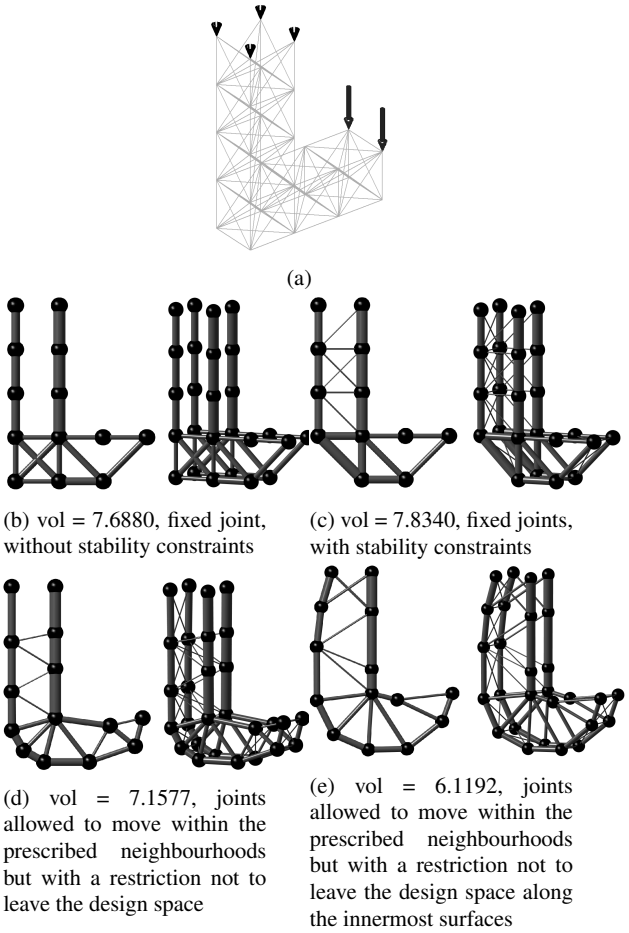

(a)

(b) vol = 7.6880, fixed joint, without stability constraints

(c) vol = 7.8340, fixed joints, with stability constraints

(d) vol = 7.1577, joints allowed to move within the prescribed neighbourhoods but with a restriction not to leave the design space

(e) vol = 6.1192, joints allowed to move within the prescribed neighbourhoods but with a restriction not to leave the design space along the innermost surfaces

Fig. 1: (a) Design domain, boundary condition, and load. (b) Side (left) and 3D (right) views the optimal design without stability constraints (c)-(e) Same views of the optimal designs with stability constraints for the problem instance in Example 1

we get the design in Figure 1e that has weight 6.1192, reduced by approximately 21% from that of the solution obtained with fixed joints in Figure 1c. As it can be seen in Figure 1e, some of the joints on the outermost edges have left the design space of Figure 1a, making the curve smoother spanning the entire outermost surfaces.

The computational statistics for all cases are presented in Table 1. The algorithm obtained the solution within a reasonable number of iterations and CPU time.

Finally, we should note that there can be seen some degree of resemblance of the optimal designs for the L-shaped problem in Figure 1e to results in [39] and [10], where there are solutions reported for geometry and topology optimization but with other types of stability constraints.

*Example 2* We solve the bridge problem of dimension $8 \times 1 \times 1$ shown in Figure 2a. The nodal loads have magnitude $(0, 0, -0.001)$, applied simultaneously, and the bound on the compliance is $\varsigma = 0.003$. When we solve the problem with and without stability constraints for fixed joints, we get the designs in Figures 2b and 2c with weights 10.3253 and 10.8904, respectively. The disjoint planar trusses in Figure 2b are now connected in Figure 2c, which is obtained by solving the problem with stability constraints. Next, we solve the problem for moving joints. First, the joints are allowed to move in a neighbourhood of radius $r = 0.4$ but restricted to remain within the design space. In this case, we get the designs in Figure 2d of weight 8.5030, that is reduced by approximately 21% compared to that of the solution of the fixed joints in Figure 2c. Moreover, we see arch structures around the top four corners. Finally, when we remove the requirement for the joints to remain in the design space, we get the solution in Figure 2e that has weight 5.7345 which is reduced by 47%, a huge saving, compared to that of the fixed joint Figure 2c. Moreover, the arch has been extended further to the upper region of the design space compared to that of the Figure 2d. The computational statistics are presented in Table 2, and once again, the method found the solution within a reasonable number of iterations and CPU time.

### 5.2 Adaptive geometry and topology optimization

Below, we describe the adaptive geometry and topology optimization technique that we have applied and some supporting numerical examples. The technique is a recursive process.

As mentioned in the introduction Section 1, and can be seen in Examples 1- 2, the designs obtained by solving the geometry and topology optimization problem (15) strongly depend on the initial configuration of the joints. The natural observation is that the designs can be improved if we allow the joints to navigate much wider regions. However, due to imposing the requirement that the joints should not come too close to each other to avoid numerical instabilities, we had to restrict the movement to smaller neighbourhoods. The aim is now to solve the problem over and over again, and obtain much better (lighter) designs. This is achieved by an iterative procedure that involves many strategies, and the overall process is motivated by [20].

First, any joints that are entirely connected to bars with cross-sectional areas below $0.001a_{\max}$, where $a_{\max}$ is the maximum attained cross-sectional area, are removed. We call these joints inactive nodes. Moreover, any joints connecting only two collinear bars of cross-sectional areas $\geq 0.001a_{\max}$ are melted, i.e., set to vanish resulting the collinear bars to merge and form a single bar. The third strategy is to merge joints that are too close to each other. In our implementation, we perform node merging if the distance between them is less than or equal to 0.25. If the nodes constitute supported or loaded joints, then the nodes are merged to these nodes.

| | Fixed joints | Moving joints | |
|---|---|---|---|
| | | Joints allowed to move within the design space | Joint allowed to move and can leave the design space except along the innermost surfaces |
| Volume | 7.8340 | 7.1577 | 6.1192 |
| IPM iter. | 76 | 76 | 88 |
| CPU(s) | 192 | 200 | 211 |

Table 1: Numerical results for the L-shaped problem in Example 1.

| | Fixed joints | Moving joints | |
|---|---|---|---|
| | | Joints allowed to move within the design space | Joint allowed to move and can leave the design space |
| Volume | 10.8904 | 8.5030 | 5.7345 |
| IPM iter. | 74 | 68 | 62 |
| CPU(s) | 412 | 401 | 370 |

Table 2: Numerical results for the bridge problem in Example 2

Otherwise, the nodes are merged to the average of the coordinates of the merging nodes. By choosing small positive values for $\varepsilon$ in (4), we determine joint dependant move limits, that is, balls of radius $r_j$ given by

$$r_j = \min\{k \min\{||\bar{v}_j - \bar{v}_p||,\ p \in I\}, 0.3\}, \tag{23}$$

where $\bar{v}_j$ and $\bar{v}_p$ are the coordinates of the joints, and $I$ is the set of indices of the joints connected to joint $j$. Moreover, we use $k = \frac{1}{3}$ except in Example 6, where we have used $k = \frac{1}{4}$. The iterative procure of the adaptive optimization stops when there is no significant change in the weight of the optimal designs, and there is no bar with length less than or equal to 0.25.

The overall use of adaptive geometry and topology optimization can also be considered as post-processing/ realization technique since designs with small number of joints and bars are achievable. The procedure is summarized in Algorithm 2.

**Algorithm 2** Adaptive geometry and topology optimization

```
Solve the problem with initial configuration of the joints.
while stopping criteria is not satisfied do
    Remove inactive nodes.
    Perform node melting.
    Perform node merging.
    Determine the size of the move limits by setting r_j as in (23).
    Solve the new problem.
end while
```

Next, we present some examples to demonstrate the benefits of the adaptive geometry and topology optimization.

*Example 3* We solve the two-dimensional problem shown in Figure 3a. It has dimension $3 \times 6$, the load is $(0, -.001)$ and the bound on the compliance is $\varsigma = 0.00025$. Initially, the radius of the move limits is set to $r = 0.3$. When we solve the problem without stability constraints, we get the optimal design shown in Figure 3b. Next, when we solve the problem with stability constraints and with the initial configuration of the joints, we get the design in Figure 3c. Now, we apply Algorithm 2 and obtain the design in Figure 3d. Repeating the process again and again, we find the designs in Figures 3e-3i. In this example, we have removed inactive nodes and performed node melting, see Figure 3d, merged too close nodes, see Figure 3h. The numerical statistics are presented in Table 3. The CPU time of the last six problem instances are shorter compared to that of the first one. This is due to the many inactive nodes and bars removed while applying adaptive optimization to the problem in Figure 3c. The designs in Figures 3d3i look similar to one of those reported in [14] obtained by solving topology optimization with buckling constraints for continuum structures.

| Stage number | Volume | IPM iter | CPU |
|---|---|---|---|
| 1 | 0.1597 | 87 | 40 |
| 2 | 0.1582 | 56 | 8 |
| 3 | 0.1574 | 55 | 7 |
| 4 | 0.1567 | 60 | 7 |
| 5 | 0.1562 | 70 | 8 |
| 6 | 0.1558 | 63 | 7 |
| 7 | 0.1554 | 56 | 7 |

Table 3: Numerical results for the two-dimensional problem in Example 3

*Example 4* We apply Algorithm 2 to the optimal design shown in Figure 1e. The results are reported in Figure 4. We have nodes merging in 4e. The final design has weight 5.8911 which has been reduced by 3.7% compared with the solution obtained at the beginning in Figure 4a. The curvature of the outer edges is smooth and with many of its joints connected to the joints in the re-entrant corner. The computational statistics are given in Table 4.

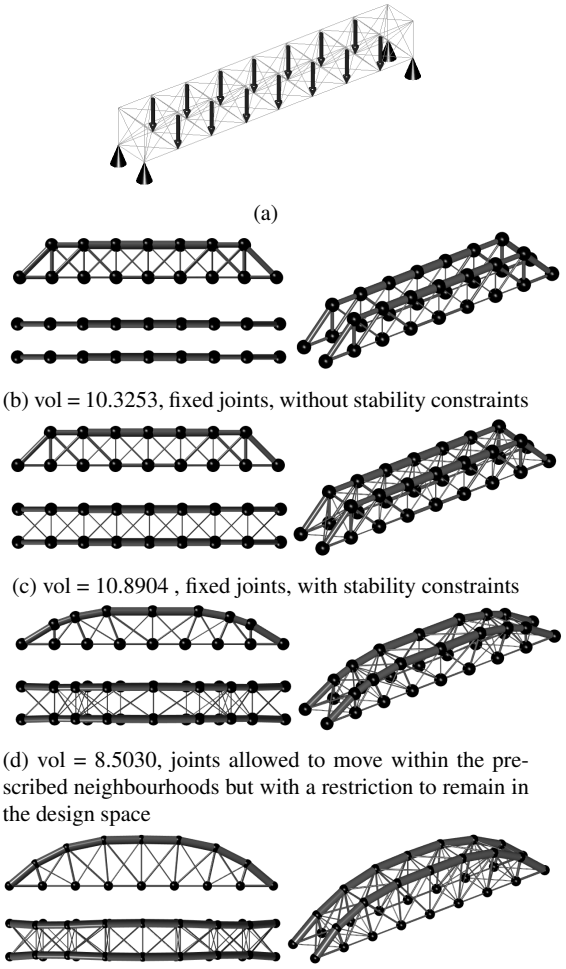

(a)

(b) vol = 10.3253, fixed joints, without stability constraints

(c) vol = 10.8904 , fixed joints, with stability constraints

(d) vol = 8.5030, joints allowed to move within the prescribed neighbourhoods but with a restriction to remain in the design space

(e) vol =5.7346, joints allowed to move within the prescribed neighbourhoods and without any restriction to remain in the design space

Fig. 2: (a) Design domain, boundary condition, and load. (b) Side (top left), top (lower left) and 3D (right) views of the optimal design without stability constraints (c)-(e) Same views of the optimal designs with stability constraints for the problem instance in Example 2.

| Stage number | Volume | IPM iter | CPU |
|---|---|---|---|
| 1 | 6.1192 | 88 | 211 |
| 2 | 5.9323 | 54 | 186 |
| 3 | 5.9075 | 71 | 190 |
| 4 | 5.9024 | 110 | 257 |
| 5 | 5.8911 | 57 | 117 |
| 6 | 5.8911 | 56 | 119 |

Table 4: Numerical results for the L-shaped problem in Example 4

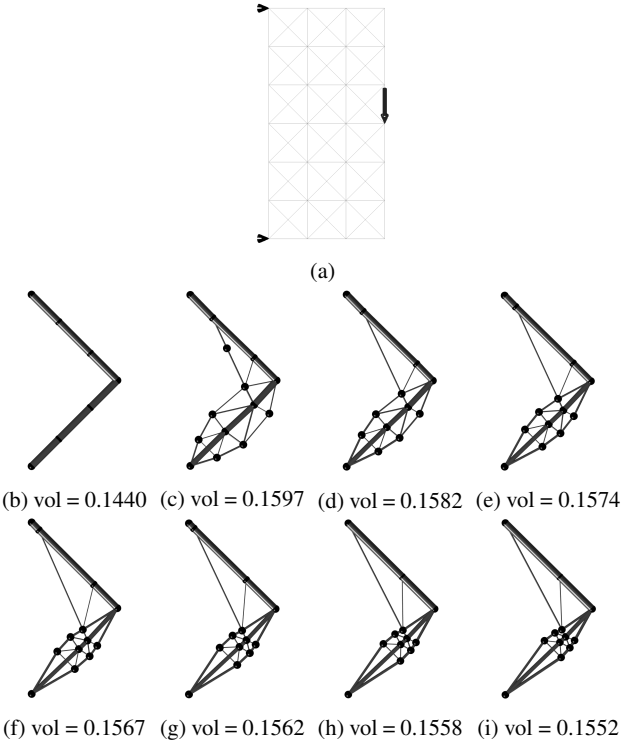

(a)

(b) vol = 0.1440 (c) vol = 0.1597 (d) vol = 0.1582 (e) vol = 0.1574

(f) vol = 0.1567 (g) vol = 0.1562 (h) vol = 0.1558 (i) vol = 0.1552

Fig. 3: (a) Design domain, boundary condition, and load. (b) Optimal design without stability constraints (c)-(i) Optimal designs with stability constraints obtained in seven stages of the adaptive optimization for the problem in Example 3

*Example 5* Here, we start with the solution of the bridge problem in Figure 2e where the top four corner nodes in the design space Figure 2a are removed. We did not have any nodes melting or merging in this case. The entire process is demonstrated in Figure 5 and Table 5. The final design in Figure 5f has weight 4.2135 which is reduced by 32% when compared to that of the solution obtained at the beginning, given in Figure 5a. Looking at the final bridge design in Figure 5f, its side-view which is a semicircular-like structure has similarity to the results in [28] and [3], which is reported for topology and geometry optimization for two-dimensional problems. Moreover, the side- and top-views show it is wider in the middle region and narrower near the two end points, is reflected in [23].

*Example 6* We solve a longer bridge problem shown in Figure 6a supported at its lower middle and end points on both edges. The dimension of the design space is $12 \times 1 \times 1$ and all of the loads have magnitude $(0, 0, -0.001)$, applied simultaneously. The bound on the compliance is set to $\varsigma = 0.005$. The problem has been solved in stages and the obtained designs are displayed in Figures 6b-6f. Once again, we see a decrease in the weight of the final design Figure 6f by 14% compared with that of the solution obtained in

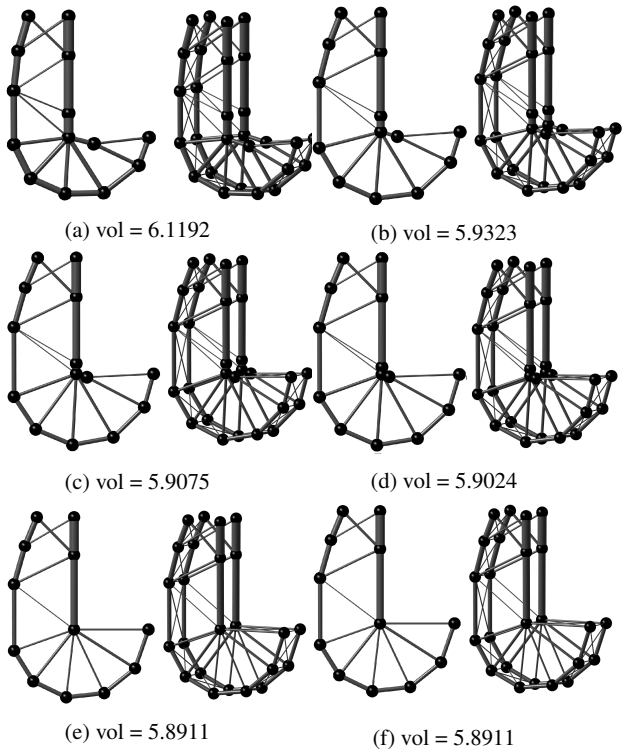


Fig. 4: Optimal designs obtained in six stages of of the adaptive optimization for the L-shaped problem in Example 4

| Stage number | Volume | IPM iter | CPU |
|---|---|---|---|
| 1 | 5.7346 | 62 | 372 |
| 2 | 4.8816 | 47 | 192 |
| 3 | 4.4699 | 47 | 201 |
| 4 | 4.2752 | 73 | 264 |
| 5 | 4.2141 | 52 | 204 |
| 6 | 4.2135 | 51 | 201 |

Table 5: Numerical results for the bridge problem in Example 5

the first stage given in Figure 6b. Looking at the final optimal design Figure 6f, the side-view can be compared to that of [28], where we have two large asymmetric semicircular-like geometries at both sides, and with a smaller symmetric curved structure in the middle. The computational results are reported in Table 6.

### 5.3 General comments based on the numerical experiments

As expected, the nonlinear semidefinite programming truss geometry and topology optimization problem given in (15) is not easy to solve. However, in most cases, by setting the value of the radius $r_i$ of the move restrictions to a reasonable value, the problems are solvable. This is because short bars are avoided. The designs can then be improved by applying

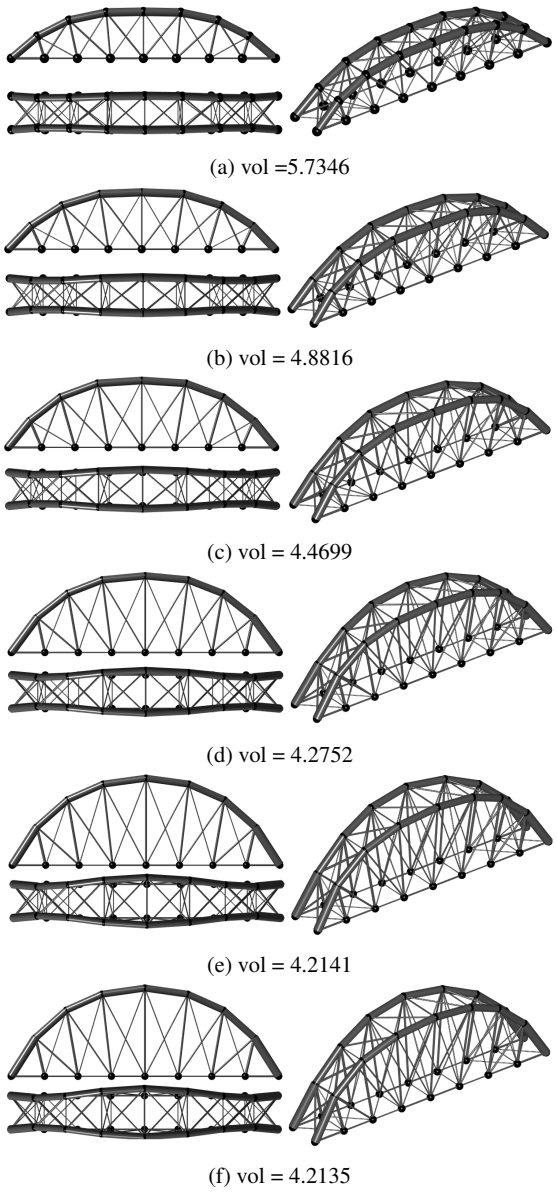


Fig. 5: Optimal designs obtained in the first six stages of the adaptive optimization for the bridge problem in Example 5

| Stage number | Volume | IPM iter | CPU |
|---|---|---|---|
| 1 | 3.6980 | 64 | 2467 |
| 2 | 3.3650 | 57 | 1046 |
| 3 | 3.2151 | 60 | 1065 |
| 4 | 3.1796 | 78 | 1387 |
| 5 | 3.1796 | 78 | 1472 |

Table 6: Numerical results for the bridge problem in Example 6

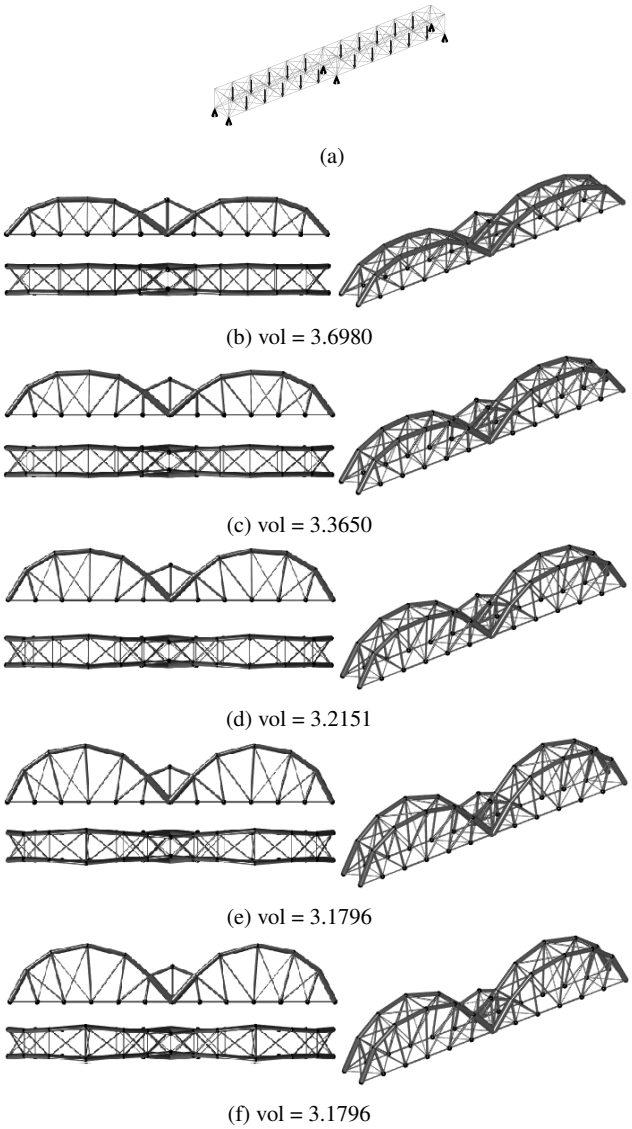


Fig. 6: (a) Design domain, boundary condition, and load. (b)-(f) Optimal designs obtained in five stages of the adaptive optimization for the bridge problem in Example 6.

the adaptive optimization procedure. There were some instances, mainly in the final stages of the adaptive optimization, when problems became harder to solve, due to an inevitable existence of short bars, see Figure 4d. However, this can be successfully resolved using a significantly less aggressive update strategy of the barrier parameter and the use of conservative step-lengths at the cost of more iterations, see Table 4. As a last comment, it is also very important that the initial point and the consequent iterations satisfy the conditions that the joints always remain within the prescribed restricted regions (2) and (3).

## 6 Conclusions

We have introduced geometry optimization to existing topology optimization with global stability constraints for truss structures, formulated as nonlinear semidefinite programming. We have demonstrated that these problems can actually be solved by a standard second-order primal-dual interior point method, despite the associated challenging mathematical properties such as nonlinearity and nonconvexity. We have applied an adaptive geometry and topology optimization to improve the quality of the optimal designs. This work is supported by several numerical experiment.
There seems to be a high degree of similarity between successive problems near the final stage of the adaptive optimization procedure. Hence, this could be a potential opportunity to use warm-start strategies [50,51] and improve the performance of the interior point method further.

## 7 Replication of results

We have provided all input and output data used in all of the examples reported in Section 5. No scaling has been involved.

## 8 Acknowledgements

The research was supported by EPSRC grant EP/N019652/1.

## References

1. Achtziger, W.: Multiple-load truss topology and sizing optimization: Some properties of minimax compliance. Journal of Optimization Theory and Applications **98**(2), 255–280 (1998)
2. Achtziger, W.: Local stability of trusses in the context of topology optimization part ii: A numerical approach. Structural optimization **17**(4), 247–258 (1999)
3. Achtziger, W.: On simultaneous optimization of truss geometry and topology. Structural and Multidisciplinary Optimization **33**(4), 285–304 (2007)
4. Achtziger, W., Bendsøe, M., Ben-Tal, A., Zowe, J.: Equivalent displacement based formulations for maximum strength truss topology design. IMPACT of Computing in Science and Engineering **4**(4), 315–345 (1992)
5. Ben-Tal, A., Bendsøe, M.P.: A new method for optimal truss topology design. SIAM Journal on Optimization **3**(2), 322–358 (1993)
6. Ben-Tal, A., Jarre, F., Kočvara, M., Nemirovski, A., Zowe, J.: Optimal design of trusses under a nonconvex global buckling constraint. Optimization and Engineering **1**(2), 189–213 (2000)
7. Ben-Tal, A., Kočvara, M., Zowe, J.: Two Nonsmooth Approaches to Simultaneous Geometry and Topology Design of Trusses, pp. 31–42. Springer Netherlands, Dordrecht (1993)
8. Bendsøe, M., Sigmund, O.: Topology Optimization: Theory, Methods and Applications. Springer (2003)
9. Bendsøe, M.P., Ben-Tal, A., Zowe, J.: Optimization methods for truss geometry and topology design. Structural optimization **7**(3), 141–159 (1994)

10. Benot Descamps, R.F.C.: The nominal force method for truss geometry and topology optimization incorporating stability considerations. International Journal of Solids and Structures **51**(13), 2390 – 2399 (2014)
11. Dobbs, M.W., Felton, L.P.: Optimization of truss geometry. ASCE J Struct Di **95**, 2015–2115 (1969)
12. Dorn, W., Gomory, R., Greenberg, H.: Automatic design of optimal structures. Journal de Mécanique **3**, 25–52 (1964)
13. Evgrafov, A.: On globally stable singular truss topologies. Structural and Multidisciplinary Optimization **29**(3), 170–177 (2005)
14. Ferrari, F., Sigmund, O.: Revisiting topology optimization with buckling constraints. Structural and Multidisciplinary Optimization **59**(5), 1401–1415 (2019)
15. Fiala, J., Kocvara, M., Stingl, M.: PENLAB: a MATLAB solver for nonlinear semidefinite optimization (2013). URL `https://arxiv.org/abs/1311.5240`
16. Gilbert, M., Tyas, A.: Layout optimization of large-scale pin-jointed frames. Engineering Computations **20**(8), 1044–1064 (2003)
17. Guo, X., Cheng, G., Olhoff, N.: Optimum design of truss topology under buckling constraints. Structural and Multidisciplinary Optimization **30**(3), 169–180 (2005)
18. Guo, X., Cheng, G., Yamazaki, K.: A new approach for the solution of singular optima in truss topology optimization with stress and local buckling constraints. Structural and Multidisciplinary Optimization **22**, 364–372 (2001)
19. Guo, X., Cheng, G., Yamazaki, K.: A new approach for the solution of singular optima in truss topology optimization with stress and local buckling constraints. Structural and Multidisciplinary Optimization **22**(5), 364–373 (2001)
20. He, L., Gilbert, M.: Rationalization of trusses generated via layout optimization. Structural and Multidisciplinary Optimization **52**(4), 677–694 (2015)
21. Imai, K., Schmit, L.A.: Configuration optimization of trusses. ASCE Journal of the Structural Division **107**(35), 745–756 (1981)
22. Jarre, F., Kočvara, M., Zowe, J.: Optimal truss design by interior-point methods. SIAM Journal on Optimization **8**(4), 1084–1107 (1998)
23. Jiang, C., Tang, C., Seidel, H., Chen, R., Wonka, P.: Computational design of lightweight trusses. CoRR **abs/1901.05637** (2019). URL `http://arxiv.org/abs/1901.05637`
24. Kirsch, U.: On singular topologies in optimum structural design. Structural Optimization **2**, 133–142 (1990)
25. Kirsch, U.: On the relationship between optimum structural topologies and geometries. Structural optimization **2**(1), 39–45 (1990)
26. Kočvara, M.: On the modelling and solving of the truss design problem with global stability constraints. Structural and Multidisciplinary Optimization **23**(3), 189–203 (2002)
27. Kočvara, M., Stingl, M.: PENNON: a code for convex nonlinear and semidefinite programming. Optimization Methods and Software **18**(3), 317–333 (2003)
28. Kocvara, M., Zowe, J.: How mathematics can help in design of mechanical structures. Pitman Research Notes in Mathematics Series pp. 76–93 (1996)
29. Levy, R., Su, H.H., Kočvara, M.: On the modeling and solving of the truss design problem with global stability constraints. Structural and Multidisciplinary Optimization **26**(5), 367–368 (2004)
30. Madah, H., Amir, O.: Truss optimization with buckling considerations using geometrically nonlinear beam modeling. Comput. Struct. **192**(C), 233–247 (2017)
31. Mela, K.: Resolving issues with member buckling in truss topology optimization using a mixed variable approach. Structural and Multidisciplinary Optimization **50**(6), 1037–1049 (2014)
32. Miguel, L.F.F., Miguel, L.F.F.: Shape and size optimization of truss structures considering dynamic constraints through modern metaheuristic algorithms. Expert Syst. Appl. **39**, 9458–9467 (2012)
33. Mitjana, F., Cafieri, S., Bugarin, F., Gogu, C., Castanié, F.: Optimization of structures under buckling constraints using frame elements. Engineering Optimization (2018)
34. Nesterov, Y.E., Todd, M.J.: Self-scaled barriers and interior-point methods for convex programming. Mathematics of Operations Research **22**(1), 1–42 (1997)
35. Nesterov, Y.E., Todd, M.J.: Primal-dual interior-point methods for self-scaled cones. SIAM Journal on Optimization **8**(2), 324–364 (1998)
36. Pedersen., P.: On the optimal layout of multi-purpose trusses. Computers and Structures **2**(2), 695–712 (1972)
37. Ringtz, U.: On topology optimization for trusses. Engineering Optimization **9**(3), 209–218 (1985)
38. Rozvany, G.I.N.: Difficulties in truss topology optimization with stress, local buckling and system stability constraints. Structural optimization **11**(3), 213–217 (1996)
39. Schwarz, J., Chen, T., Shea, K., Stanković, T.: Efficient size and shape optimization of truss structures subject to stress and local buckling constraints using sequential linear programming. Structural and Multidisciplinary Optimization **58**(1), 171–184 (2018)
40. Sergeyev, O., Pedersen, P.: On design of joint positions for minimum mass 3d frames. Structural optimization **11**(2), 95–101 (1996)
41. Sokół, T., Rozvany, G.I.N.: On the adaptive ground structure approach for multi-load truss topology optimization. In: 10th World Congresses of Structural and Multidisciplinary Optimization (2013)
42. Stingl, M.: On the solution of nonlinear semidefinite programs by augmented Lagrangian method. Ph.D. thesis, Institute of Applied Mathematics II, Friedrich-Alexander University of Erlangen-Nuremberg (2006)
43. Stolpe, M., Svanberg, K.: On the trajectories of the epsilon-relation relaxation approach for stress-constrained truss topology optimization. Structural and Multidisciplinary Optimization **21**, 140–151 (2001)
44. Stolpe, M., Svanberg, K.: A note on tress-based truss topology optimization. Structural and Multidisciplinary Optimization **25**, 62–64 (2003)
45. Svanberg, K.: Optimization of geometry in truss design. Computer Methods in Applied Mechanics and Engineering **28**(1), 63 – 80 (1981)
46. Tejani, G.G., Savsani, V.J., Patel, V.K., Savsani, P.V.: Size, shape, and topology optimization of planar and space trusses using mutation-based improved metaheuristics. Journal of Computational Design and Engineering **5**(2), 198 – 214 (2018)
47. Torii, A.J., Lopez, R.H., Miguel, L.F.F.: Modeling of global and local stability in optimization of truss-like structures using frame elements. Structural and Multidisciplinary Optimization **51**(6), 1187–1198 (2015)
48. Tugilimana, A., Filomeno Coelho, R., Thrall, A.P.: Including global stability in truss layout optimization for the conceptual design of large-scale applications. Structural and Multidisciplinary Optimization **57**(3) (2018)
49. Tyas, A., Gilbert, M., Pritchard, T.: Practical plastic layout optimization of trusses incorporating stability considerations. Comput. Struct. **84**(3-4), 115–126 (2006)
50. Weldeyesus, A.G., Gondzio, J.: A specialized primal-dual interior point method for the plastic truss layout optimization. Computational Optimization and Applications **71**(3), 613–640 (2018)
51. Weldeyesus, A.G., Gondzio, J., He, L., Gilbert, M., Shepherd, P., Tyas, A.: Adaptive solution of truss layout optimization problems with global stability constraints. Structural and Multidisciplinary Optimization (2019). DOI 10.1007/s00158-019-02312-9
52. Weldeyesus, A.G., Stolpe, M.: A primal-dual interior point method for large-scale free material optimization. Computational Optimization and Applications **61**(2), 409–435 (2015)

53. Yamashita, H., Yabe, H.: A survey of numerical methods for nonlinear semidefinite programming. Journal of the Operations Research Society of Japan **58**(1), 24–60 (2015). DOI 10.15807/jorsj.58.24
54. Yamashita, H., Yabe, H., Harada, K.: A primal-dual interior point method for nonlinear semidefinite programming. Mathematical Programming **135**(A), 89–121 (2012)
55. Zhang, Y.: On extending some primal-dual interior-point algorithms from linear programming to semidefinite programming. SIAM Journal on Optimization **8**(2), 365–386 (1998)
56. Zhou, M.: Difficulties in truss topology optimization with stress and local buckling constraints. Structural optimization **11**(2), 134–136 (1996)